


## Review

# The Neglected Involvement of Organic Matter in Forming Large and Rich Hydrothermal Orogenic Gold Deposits

Damien Gaboury 

Laboratoire de Métallogénie Expérimentale et Quantitative (LAMEQ), Université du Québec à Chicoutimi (UQAC), 555 Boulevard de l'Université, Chicoutimi, QC G7H 2B1, Canada; dgaboury@uqac.ca

**Abstract:** Orogenic gold deposits have provided most of gold to humanity. These deposits were formed by fluids carrying dissolved gold at temperatures of 200–500 °C and at crustal depths of 4–12 km. The model involves gold mobilization as  $\text{HS}^-$  complexes in aqueous solution buffered by  $\text{CO}_2$ , with gold precipitation following changes in pH, redox activity ( $f\text{O}_2$ ), or  $\text{H}_2\text{S}$  activity. In this contribution, the involvement of carbonaceous organic matter is addressed by considering the formation of large and/or rich orogenic gold deposits in three stages: the source of gold, its solubilization, and its precipitation. First, gold accumulates in nodular pyrite within carbonaceous-rich sedimentary rocks formed by bacterial reduction of sulfates in seawater in black shales. Second, gold can be transported as hydrocarbon-metal complexes and colloidal gold nanoparticles for which the hydrocarbons can be generated from the thermal maturation of gold-bearing black shales or from abiotic origin. The capacity of hydrocarbons for solubilizing gold is greater than those of aqueous fluids. Third, gold can be precipitated efficiently with graphite derived from fluids containing hydrocarbons or by reducing organic-rich rocks. Black shales are thus a key component in the formation of large and rich orogenic gold deposits from the standpoints of source, transport, and precipitation. Unusual  $\text{CO}_2$ -rich,  $\text{H}_2\text{O}$ -poor fluids are documented for some of the largest and richest orogenic gold deposits, regardless of their age. These fluids are interpreted to result from chemical reactions involving hydrocarbon degradation, hence supporting the fundamental role of organic matter in forming exceptional orogenic gold deposits.

**Keywords:** orogenic gold deposits; carbonaceous organic matter; hydrocarbons; graphite;  $\text{CO}_2$ -rich fluids



**Citation:** Gaboury, D. The Neglected Involvement of Organic Matter in Forming Large and Rich Hydrothermal Orogenic Gold Deposits. *Geosciences* **2021**, *11*, 344. <https://doi.org/10.3390/geosciences11080344>

Academic Editors:  
Jesus Martinez-Frias and  
Gianluca Groppelli

Received: 14 May 2021  
Accepted: 13 August 2021  
Published: 17 August 2021

**Publisher's Note:** MDPI stays neutral with regard to jurisdictional claims in published maps and institutional affiliations.



**Copyright:** © 2021 by the author. Licensee MDPI, Basel, Switzerland. This article is an open access article distributed under the terms and conditions of the Creative Commons Attribution (CC BY) license (<https://creativecommons.org/licenses/by/4.0/>).

## 1. Introduction

For at least 6000 years, the use of gold [1] marked a change for humanity: the use of metals. Gold was the first metal used because it occurs in a native form. Gold is insoluble under surface conditions and non-oxidable, so its physical properties are conserved. Presenting a shining yellowish color like that of the sun and exhibiting extreme malleability, gold was first used for ornamental purposes and later as a medium of exchange and coinage. The first exploitations were from rivers or dried riverbeds, where gold was physically concentrated as nuggets. Later, gold was extracted from quartz vein outcroppings at surfaces. Both types of gold extraction are still in use today.

Humans have always had a fascination and irrational relationship with gold. Gold was and is still a physical means for conserving values (e.g., [2]). Consequently, wars, invasions, colonizations, and territorial conquests (gold rushes) were established and driven. Gold, as has any other substance, positively and negatively impacted human development. Artisanal gold extractions are still providing revenue for 15–20 million persons worldwide [3], whereas hundreds of mines are producing gold commercially in more than 42 countries ([www.gold.org](http://www.gold.org) (accessed on 21 March 2021)).

In the inorganic world of metals, minerals, and rocks, consideration of the roles of organic matter in accumulating, solubilizing, and precipitating gold in lodes was not a natural way of thinking for geologists. At first, it may appear paradoxical that the

ultimate noble metal requires organic matter for concentration. In this contribution, I address recent advances regarding the role of carbon-rich organic matter in forming rich and large gold deposits in three stages: (1) the source stage, when gold in seawater accumulates in organic-rich sediments; (2) the mobilization stage, when gold is solubilized by hydrocarbon-metal complexes and colloidal nanoparticles for hydrothermal transport along faults; and (3) the precipitation stage. It is demonstrated that unusual CO<sub>2</sub>-rich, H<sub>2</sub>O-poor fluids, documented for some of the largest and richest orogenic gold deposits, are the result of chemical reactions involving hydrocarbon degradation, hence demonstrating the fundamental role of carbonaceous organic matter.

## 2. Orogenic Gold Deposits

“Gold is where you find it” was the adage used for explaining occurrences of gold. Decades of research has provided a better understanding of the distribution of gold deposits in space and time and the physicochemical processes involved in their formation (e.g., [4–7]). Approximately 75% of gold extracted by humanity [8] comes from a genetic type called “orogenic gold deposit” [9]. Gold primarily occurs in quartz-bearing veins (Figure 1), formed at depths between 4 and 12 km and with temperatures ranging from 200 to 500 °C; these are hosted in metamorphic volcano-sedimentary belts. Gold is typically the only metal extracted economically, but silver can be a by-product, and Au/Ag ratios range from 5 to 10 [10]. Typical gold grades are in the range of 4–8 ppm Au [11], and deposit sizes range from tonnes to hundreds of tonnes of in-situ gold.

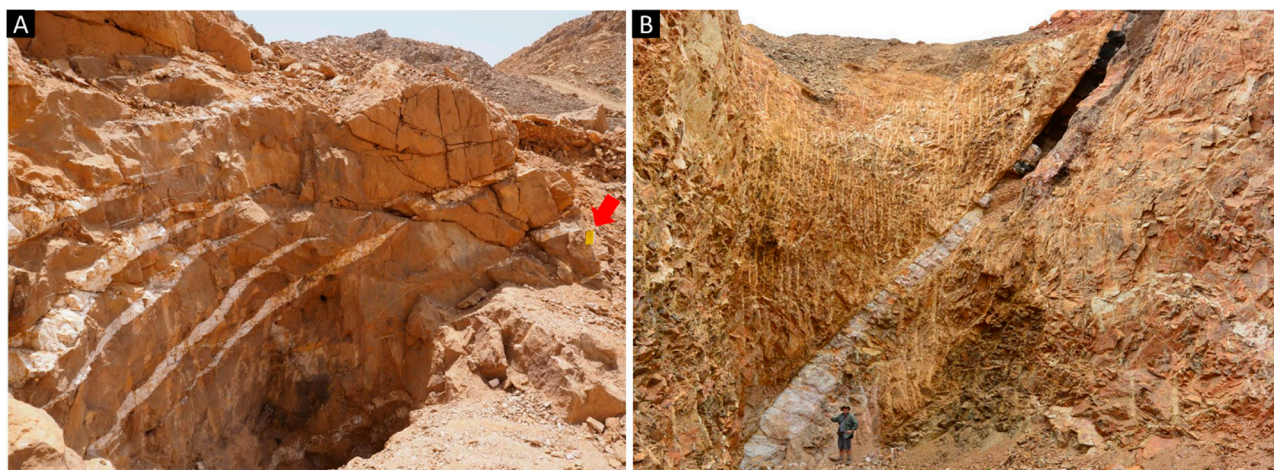


**Figure 1.** Typical aspect of orogenic gold-bearing quartz veins, with low sulfide content and a strong iron-carbonate alteration, inducing an orange tint to the host rocks. (A) Extensional, en echelon, low-dipping quartz vein network developed in a competent rock bordered by shear zones, New Rock mine, Sudan. Yellow field book (red arrow) as scale (20 cm). (B) Laminated quartz vein hosted in a reverse shear zone, Negeim mine, Sudan.

Orogenic gold deposits are hosted in accretionary or collisional orogens, ranging in age from Meso-Archean to tertiary times. Modern analogues are presently forming at depth, such as along the Alpine Fault in New Zealand [12]. These orogens, commonly termed greenstone belts, are composed mostly of oceanic rocks, such as basaltic lavas and sedimentary rocks. Although orogens cover the entire geological age spectrum [13], orogenic gold deposits are distributed in three main periods (Figure 2; [14,15]): (1) Neoarchean (2.75–2.55 Ga); (2) Paleoproterozoic (2.1–1.75 Ga), (3) and Neoproterozoic-Phanerozoic (<800 Ma)).

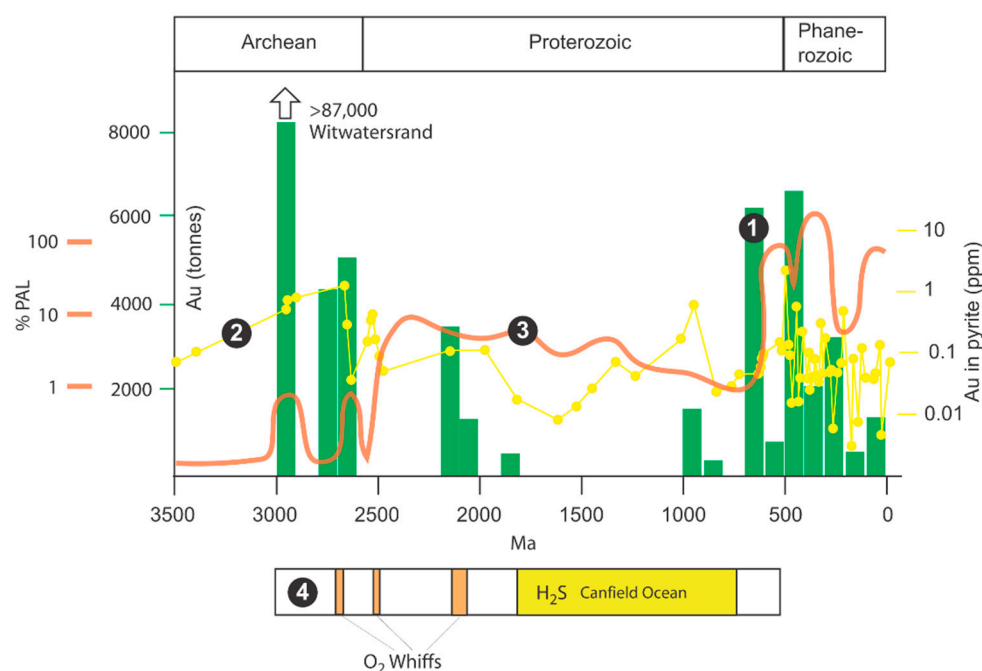


**Figure 2.** Secular distribution of the orogenic gold deposits (1—[16]) in relation to gold contents of nodular pyrites from black shales (2—geometric mean of LA-ICP-MS analyses from time interval: [16]), an estimate of oxygenation based on Se content of nodular pyrite, expressed as a percentage of present atmosphere level (% PAL—3—[17]), and O<sub>2</sub> whiffs and Canfield ocean (4—[18]). The high levels of Au in black shales correspond to the greatest periods for orogenic gold deposit formation. The lack of Au deposits between 1800 and 800 Ma (the boring period) is correlated to low levels of Au in the oceans, corresponding to the Canfield ocean. Higher gold values in black shales match the surges of atmospheric O<sub>2</sub> and the documented O<sub>2</sub> whiffs, suggesting that gold was leached from continents and was more soluble in seawater for better accumulation in black shales. This evidence supports a model in which oceanic gold was deposited with carbonaceous organic matter and trapped in nodular seafloor pyrites to constitute Au-enriched source rocks.

The orogenic gold model, recently reviewed by Gaboury [6], involves (1) fluid generation at depth by metamorphic dehydration of ocean-derived rocks at the transition to amphibolite facies [4] during orogen formations, (2) the extraction of gold from sedimentary pyrite during pyrrhotite conversion [19–22], and (3) an excess of sulfur in solution [23], which is used for carrying gold as HS<sup>−</sup> aqueous complexes [24] under neutral pH and reducing conditions buffered by dissolved CO<sub>2</sub> [25]. Gold-bearing metamorphic fluids are channeled upward along faults, from the dehydration zone to the precipitation site in the upper crust, which is commonly under greenschist facies conditions. These concepts are detailed below in discussions of the roles of carbonaceous organic matter.

Nonetheless, other deeply sourced fluids have been considered, such as those from oceanic crust and sediment devolatilization in subduction zones or from overlying fertilized mantle lithosphere [5,7,26,27]. Magmatic fluids can also form gold deposits, which are not interpreted as orogenic but are considered intrusion-related gold systems (IRGSs: [28]). In some particular cases, gold-bearing magmatic fluids can be mixed with metamorphic fluids to form orogenic gold deposits (e.g., [29]).

### 3. Fluid Composition and Generation

The fluid composition of orogenic gold deposits was estimated from the study of fluid inclusions for more than 70 years (e.g., [30,31]). Hundreds of studies have detailed the mineralizing fluids from worldwide examples covering all ages (e.g., [32]). The fluids are aqueous with low salinity (<5 wt% NaCl equiv.), ubiquitous CO<sub>2</sub>, and variable contents of N<sub>2</sub>, CH<sub>4</sub>, and, in some cases, H<sub>2</sub>, C<sub>2</sub>H<sub>6</sub>, H<sub>2</sub>S, He, and Ar. Thermodynamic calculations

have demonstrated that metamorphic dehydration of seafloor rocks is a viable mechanism for producing abundant aqueous-carbonic and low-salinity fluids. Elmer et al. [33] and Phillip and Powell [4] demonstrated that seafloor rocks, hydrated initially by hydrothermal seawater convection cells at oceanic ridges [34], release fluids at the metamorphic transition of greenschist to amphibolite, mostly when chlorite is converted to amphibole. Metamorphic fluids have a more diverse volatile composition than other fluids, such as seawater, magmatic fluids, or meteoric fluids, because they are generated by devolatilization of lithologies, where organic compounds in sedimentary rocks contribute to C-O-H-S-N contents [35].

Of particular interest, CO<sub>2</sub>-rich and H<sub>2</sub>O-poor fluid inclusions have been documented from some world-class gold districts and deposits (Table 1), such as those at the Red Lake [36], Ashanti [37] and Tarkwa goldfields [38], and the Detour Gold and Wona deposits [35]. Fluids for these deposits also contain CH<sub>4</sub>, N<sub>2</sub>, and C<sub>2</sub>H<sub>6</sub> (Table 1). The origins of these fluids are still debated (e.g., [30,35]).

**Table 1.** Selected examples of large and/or rich gold orogenic gold deposits.

Deposit/District	Au ppm	Moz	CH <sub>4</sub>	C <sub>2</sub> H <sub>6</sub>	Age	Country	Status	Remark	Reference
Campbell-Red Lake mine	20	25	X	?	Archean	Canada	Production	One of the world richest gold mine	[36]
Detour Gold mine	1	20	X	X	Archean	Canada	Production	The largest Canadian gold deposit	[35]
HGZ (Perron) *	>30	?	X	X	Archean	Canada	Exploration	One of the richest gold deposits not mined	[39]
Wona Mine (Mana district)	5	10	X	X	Paleoproterozoic	Burkina Faso	Production	The most gold endowed district in Burkina Faso	[35]
Ashanti-Obuasi mine	8	70	X	?	Paleoproterozoic	Ghana	Production	The largest Birimian gold deposit	[37,40]
Tarkwa mine	?	20	X	?	Paleoproterozoic	Ghana	Production	One of the largest gold mines in Ghana	[38,41]
Gabgaba district **	2	>5	X	X	Neoproterozoic	Sudan	Production	The largest East Africa gold project	[42]
Macrears mine	1	10	X	X	Cretaceous	New Zealand	Production	One of the world largest single Phanerozoic deposit	[43]

\* Mineral resource estimation in preparation. \*\* New emerging district under intensive exploration: Moz estimated.

For the Ashanti gold belt, Goldfarb et al. [44] suggested that devolatilization of abundant carbonaceous schists and cherts could lead to a variety of carbon-bearing molecular components within metamorphic C-O-H-S fluids bearing gold. Such a sedimentary source is confirmed by the compositions of stable carbon isotopic mixture in quartz-hosted, CO<sub>2</sub>-rich fluid inclusions [45]. These unusual fluids are thus likely derived from the metamorphism of carbonaceous-rich sedimentary rocks. Nonetheless, these fluids are associated with either very high-grade or very large gold deposits (Table 1), suggesting that CO<sub>2</sub>-rich and H<sub>2</sub>O-poor fluids have unrecognized potential for forming exceptional orogenic gold deposits.

#### 4. Sources of Gold

The sources of gold for orogenic deposits have been reviewed by numerous authors (e.g., [6,26,46]). Gold can be sourced from intrusion degassing (e.g., [47]) and oceanic basalt devolatilization (e.g., [48–50]). However, carbonaceous- and pyrite-rich sedimentary rocks,



commonly referred to as black shales, are considered one of the most important sources (e.g., [6,8,19,21,42,43,51,52]).

Gold and other trace metals occurring in sedimentary pyrite can be liberated by recrystallization and hydrothermal replacement processes occurring under metamorphic conditions, corresponding to the pyrite–pyrrhotite transition [19,21,22,53,54]. Gold concentrations in nodular pyrite average 0.09 ppm [16] but can reach 10 ppm Au in orogenic gold districts (e.g., [29,55,56]). Considering that nodular pyrite can constitute up to 20% of black shales and that black shales are very extensive marine sediments, these rocks may constitute a significant volume for providing gold. In addition, because pyrrhotite ( $\text{Fe}_{1-x}\text{S}$ ) has a lower S content (37.67% vs. 53.45%) than pyrite ( $\text{FeS}_2$ ), the conversion can also provide S in solution for solubilizing gold [23]. Gaboury [6] stated that, in addition to gold, fluids and ligands ( $\text{HS}^-$ ) can all be sourced from the metamorphism of black shales and associated rocks under amphibolite conditions.

Using a solid-probe mass spectrometer system [57], Gaboury [35] documented that ethane ( $\text{C}_2\text{H}_6$ ) is present in fluid inclusions from orogenic gold deposits, ranging in age from ~2800 Ma to ~100 Ma. Ethane is sourced from thermally degraded organic matter because the values of  $\text{CH}_4/(\text{C}_2\text{H}_6 + \text{C}_3\text{H}_8)$ , expressed as  $\text{C}_1/\text{C}_{2+}$  in hydrothermal fluids, are lower than 100 [58]. Consequently, ethane provides a reliable tracer for the involvement of carbonaceous and pyritic shales at depth in the formation of gold deposits [35].

The ultimate support for a sedimentary gold source model is provided by the link between gold dissolved in oceans and the temporal distribution of orogenic gold deposits (Figure 2). This was first proposed by Tomkins [15] and later documented by Large et al. [16] by using gold concentrations in primary pyrites from black shales. Oxidizing seawater conditions are favorable for gathering gold in nodular sedimentary pyrite in black shales [16]. The lack of major orogenic gold deposits from the middle to late Proterozoic (~1800 to 800 Ma—the boring period) is interpreted as being related to low levels of Au in the oceans [16]. During this period, the deep oceans were anoxic and sulfidic [59], hence limiting the bacterial reduction of sulfate and the incorporation of gold in primary pyrite [6]. The occurrence of orogenic gold deposits in Neoproterozoic time (Figure 2), such as those in Sudan, which also contain ethane [42], coincides with the reappearance of oxygenic conditions in the oceans [16,60].

In addition to gold in nodular pyrite, Zhong et al. [53] demonstrated that metamorphic devolatilization of sulfur-rich pelites, essentially by chlorite dehydration, can liberate ~2 ppb of gold in autogenous fluids after crossing the greenschist–amphibolite facies boundary. Recent work by Wu et al. [54] demonstrated that carbonaceous matter, interstitial to framboidal pyrite in black shales, also contains As and Au accumulated during biological activity, which are released during metamorphic recrystallization and hydrothermal replacement.

All this evidence supports a model in which gold in oceans was the source for later remobilization in orogenic gold-bearing veins during tectonic shortening and related metamorphism [61]. Gold was accumulated in organic-rich sediments from the bacterial reduction of sulfate [62] and incorporation in primary nodular pyrites and carbonaceous organic matter (Figure 3A).

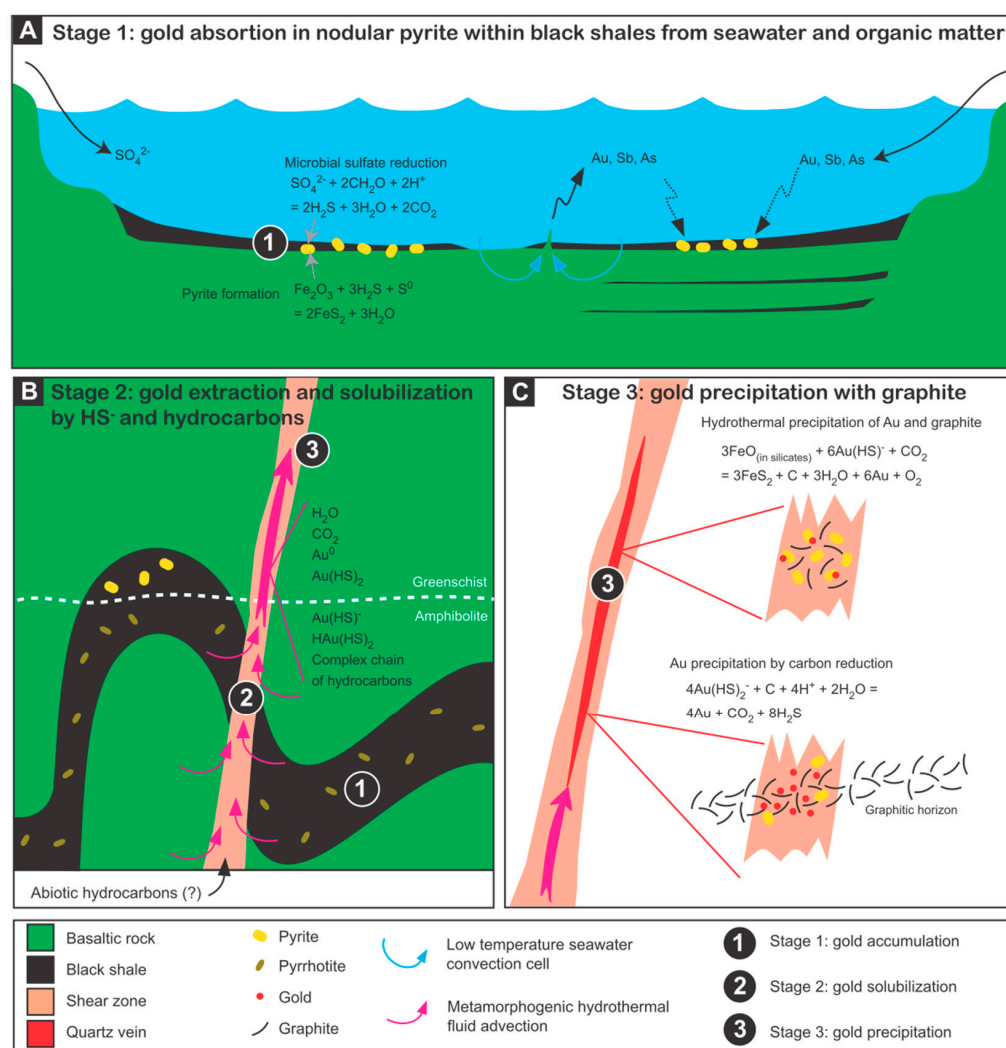


**Figure 3.** Schematic representation of the role of carbonaceous organic matter in the formation of orogenic gold deposits in three stages. (A) Source stage when gold in seawater accumulates in primary pyrites from the bacterial reduction of sulfate in organic material-rich sediments; modified from Rickard et al. [62]. (B) Mobilization stage when gold is solubilized by hydrocarbon-metal complexes and as colloidal gold nanoparticles for hydrothermal transport along faults following basin inversion and related tectonic shortening and metamorphism. Hydrocarbons are generated by thermal maturation of black shales or from abiotic deep contributions. (C) Precipitation stage when gold is co-precipitated with graphite from hydrocarbon-rich fluids or when gold is precipitated by carbon-rich reducing horizons.

## 5. Gold Solubility

Gold is a noble metal, and its solubilization for hydrothermal transport thus requires a ligand to enhance its solubility. Experiments performed at high temperatures (500 °C) and pressures (500 bar) have confirmed that gold is soluble as  $\text{HS}^-$  complexes in aqueous solution (e.g., [24,63]). Gold solubility is a function of oxygen fugacity ( $f\text{O}_2$ ) and pH. The highest solubility occurs at a pH close to the neutral value (pH ~ 7) and at  $f\text{O}_2$  just below the oxide-sulfide mineral stability boundary [64]. Depending on the amount of sulfur in solution and the temperature, the maximal gold solubility can reach 100 to 1200 ppb, values confirmed by the analyses of individual aqueous fluid inclusions by LA-ICP-MS [65–67]. However, Simmons et al. [64] recently demonstrated that the maximal solubility of gold is reached at temperatures >350 °C because the concentration of aqueous S is reduced by

fluid-rock buffering at lower temperatures. This buffering parameter was neglected in previous experiments.

The association between carbonaceous matter and gold has been observed for a long time (e.g., [68]). More recently, hydrocarbons have been invoked for the formation of gold deposits, especially those in sedimentary settings that were formed at low temperatures, such as epithermal [69], Carlin-type [70,71], and even the giant Witwatersrand goldfields [72–74]. Petroleum-phase gold transport is now considered a potentially efficient ore-forming process based on experimental data [75,76], but specific Au-organic/Au-hydrocarbon complexes remain to be identified. Within hydrocarbon-rich fluids, gold can also be transported as colloidal nanoparticles [77–79]. Experiments have demonstrated that the solubilities of Au and Zn in natural crude oils are higher than those in aqueous solutions with typical  $\text{HS}^-$  concentrations [80]. Gold solubility reached ~50 ppb at 250 °C in crude oils [80], which is 5 to 50 times higher than the aqueous solubility. The maximal solubility for Zn reached ~25 ppm at 200 °C [80], which is approximately 100 times higher than the aqueous solubility in low-chloride solutions [81].

If petroleum has the ability to solubilize gold, its direct involvement in carrying gold in natural mineralizing systems remains to be demonstrated. Because all orogenic gold deposits, even those bearing  $\text{CO}_2$ -rich fluids, contain aqueous fluids in their inclusions, it is difficult to exclude the aqueous transport of gold. The ultimate demonstration would come from an orogenic gold deposit with fluid inclusions devoid of water. The High-Grade Zone (HGZ) of the Perron gold deposit in the Archean Abitibi belt in Canada provides such a demonstration [39]. The HGZ is characterized by coarse visible gold disseminated in quartz veins with ~5% sphalerite, a zinc-bearing sulfide ([Zn, Fe]S). Gold grades range between 30 and 300 ppm, 10 to 50 times higher than typical grades [11], and are coherently distributed along a steeply plunging >1.2 km-long ore shoot. Gold mineralization occurred at ~370 °C, well below and later than the metamorphic peak of ~600 °C recorded by the host rocks. Fugacity of sulfur (−6) and oxygen (−28), and pH (~7) are within the range for providing the best conditions at a temperature of 350 °C for solubilizing gold.

Fluid inclusions are rich in hydrocarbon-bearing volatiles ( $\text{CH}_4$ ,  $\text{C}_2\text{H}_6$ ), with variable concentrations of  $\text{CO}_2$ ,  $\text{N}_2$ , noble gases ( $\text{N}_2$ , He, and Ar), and  $\text{H}_2\text{S}$ . Butane and possibly propane were detected in the mineralizing fluids, as were other organic compounds that remain to be identified. Comparatively, these fluids are similar to fossil gas from producing fields, although richer in  $\text{CO}_2$ . The lack of water implies that Au and Zn were not transported as aqueous species even if the aqueous solubility of gold was optimal. Indeed, Gaboury et al. [39] concluded that gold and zinc were transported as hydrocarbon-metal complexes and as colloidal gold nanoparticles, hence accounting for the exceptional concentration of gold and zinc for an orogenic gold deposit.

The Archean Perron example raises the following question: is hydrocarbon-phase gold transport important for the formation of other rich and large gold deposits?  $\text{CO}_2$ -rich and  $\text{H}_2\text{O}$ -poor fluid inclusions from some world-class gold districts and deposits also contain methane and ethane (Table 1). These cases emphasize the possibility that hydrocarbon-phase gold solubilization and colloidal gold transport was not recognized as a fundamental parameter for the formation of important gold deposits and districts (Figure 3B). Since gold can be extracted from carbonaceous-rich, pyrite-bearing black shales, hydrocarbons can thus be sourced from the same rocks by thermal maturation of organic matter [35].

## 6. Gold Precipitation

The solubility of gold is strongly dependent on redox conditions for gold transported in solution as  $\text{HS}^-$  complexes. Carbonaceous matter plays two roles in precipitating gold; it serves as a reducing agent in both the host rocks and in the mineralizing fluids.

Fluid reduction in the presence of carbon in the host rocks is a documented mechanism (Figure 3C), analogous to the role of activated carbon in the carbon-in-pulp processing plants for commercial gold recovery. This precipitation effect was proposed for the giant Witwatersrand goldfield [82], where approximately 50% of gold is associated with

elemental carbon, either as carbon seams, veinlets, or nodules. Recently, Fuchs et al. [74] proposed a detailed mechanism for the Witwatersrand goldfield: the liquid, gaseous, and solid hydrocarbons in the reefs acted as efficient chemical traps for the concentration of gold by reducing the redox state of the fluids leading to a drastic drop of the aqueous solubility of gold.

Alternatively, carbonaceous matter may be deposited from hydrothermal fluids, which would account for its coexistence with pyrite, as commonly observed in natural gold-bearing samples [83]. Carbonaceous matter in ore was considered important for gold deposition, but its role was not well understood until recently. Indeed, Hu et al. [84] demonstrated by thermodynamic modelling that carbonaceous matter and pyrite were co-deposited, mainly from ore fluids. Gold precipitates when deposition of pyrite and carbonaceous matter decreases  $\text{H}_2\text{S}$  concentrations in ore fluids and destabilizes  $\text{Au}(\text{HS})^-$  complexes (Figure 3C). Carbonaceous matter, occurring mostly as graphite, is deposited from  $\text{CO}_2$  and  $\text{CH}_4$  in ore fluids. Such a graphitization process related to gold precipitation is confirmed by the occurrence of  $\text{H}_2$  in ore fluids. Gaboury et al. [43] demonstrated that the occurrence of  $\text{H}_2$ , as the second most abundant compound after water, found with  $\text{CO}_2$ , is the result of reactions consuming  $\text{C}_2\text{H}_6$ ,  $\text{CO}_2$ , and  $\text{CH}_4$  to produce graphite associated with gold mineralization in the Otago Schist belt.

## 7. The Fundamental Involvement of Organic Matter

Therefore, the roles of carbonaceous matter appear fundamental for (1) concentrating gold in organic-rich sediments by bacterial reactions, (2) solubilizing gold as hydrocarbon-phase metal and colloidal gold nanoparticles during the hydrothermal remobilization of gold in lodes and veins, and (3) precipitating gold (Figure 3). Carbonaceous- and pyritic-rich shales would provide gold, HS ligands, and fluids, in addition to various organic C-H-N-S compounds, having the potential to enhance the gold carrying capacity of mineralizing fluids. Furthermore, hydrocarbons in the fluids may enhance gold precipitation with graphite.

For gold sourced from organic-rich pyrite-bearing shales, all three of the reviewed processes could operate sequentially to form orogenic gold deposits.

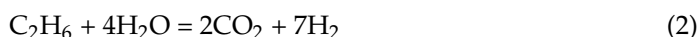
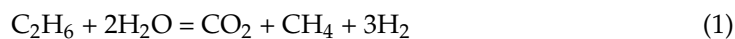
However, in the prograde metamorphic context, it seems unlikely that black shales would provide hydrocarbon gases, as the organic matter would have been transformed in graphite and semi-graphite before reaching the greenschist/amphibolite facies boundary [85]. One possible explanation for generating hydrocarbon-bearing fluids lies in the late metamorphic thermal rebound model [6]. In this model, fluids are generated late during the exhumation after the rapid burial of rocks induced by the regional tectonic shortening. Buried cooler, hydrated, and organic matter-bearing rocks are later overprinted by thermal isograd rebound and re-equilibration of the newly formed crust. This model is coherent with the late origin of orogenic gold deposits [10].

The recent study of the Witwatersrand basin [74] also provides support to the possibility of having hydrocarbons at temperatures higher than the oil window (60–150 °C) reached during diagenesis and catagenesis (e.g., [86]). Hydrocarbon gases and minor oils were involved during hydrothermal gold precipitation at a temperature of  $350 \pm 50$  °C [74], whereas oil, gas, and bitumen are interpreted to be sourced mostly from underlying black shale units [73,74].

Conversely, abiotic hydrocarbons (e.g., [87,88]; Figure 3B) may enhance gold solubility by forming organic-gold complexes or facilitating colloidal transport, regardless of the gold source, as proposed for the HGZ [39]. Nevertheless, the importance of organic matter for forming orogenic gold deposits is a relatively new concept, and this is especially true for gold transport by hydrocarbon-rich fluids. Re-assessments of numerous gold deposits, especially those with unusual  $\text{CO}_2$ -rich and  $\text{H}_2\text{O}$ -poor fluid inclusions (Table 1), are thus necessary.



Hydrothermal reactions involving the consumption of water and C<sub>2</sub>H<sub>6</sub>, the ultimate proxy for the involvement of gold-bearing carbonaceous matter at depth [35], account for CO<sub>2</sub>-rich, H<sub>2</sub>O-poor fluids, as follows:



Ethane and methane are also common constituents of CO<sub>2</sub>-rich fluids (Table 1). In addition, the presence of H<sub>2</sub> in the mineralizing fluids in the Otago Schist [43] confirms that the chemical reactions (Equations (1) and (2)) are viable for the ultimate production of CO<sub>2</sub>-rich, H<sub>2</sub>O-poor fluids. Consequently, if these unusual fluids result from hydrocarbon consumption, then hydrocarbons may be indicative of (1) a favorable sedimentary source for gold, (2) enhanced gold solubility involving hydrocarbon-metal complexes and colloidal gold, and (3) efficient gold precipitation with graphite.

Although the genetic roles of organic matter were previously underestimated, the geological settings are supportive. The Witwatersrand goldfield, the largest in the world, is hosted along the margins of a very large Archean sedimentary basin (300 km × 100 km), with >4.5 km thick shales and argillites at its base [82]. The Giant Muruntau mine, the largest single orogenic gold deposit, with >5300 T Au (>170 Moz Au), is hosted in iron-rich and carbonaceous Ordovician to Early Silurian marine clastic rocks [89,90]. The Palaeoproterozoic Birimian belts of Western Africa comprise abundant graphitic shales rich in nodular gold-bearing pyrite [29]. These belts showed the highest rates of discovery of significant (>1 Moz Au/31 tonnes) deposits in the last decade [44]. The largest Palaeozoic goldfields are primarily hosted in sedimentary sequences, including the Victorian (Australia) and Mother Lode (CA, USA) districts.

## 8. Concluding Remarks

Why did it take so long for the importance of organic compounds for forming important orogenic gold deposits and districts to be realized? Numerous explanations can be provided. In comparison, most other types of hydrothermal metal deposits were formed by fluids originating from a well-defined source, such as seawater, magmatic degasification, or surficial water (e.g., [91]). Inorganic ligands, such as Cl<sup>−</sup> (seawater), halides (Cl<sup>−</sup>, F<sup>−</sup>, Br<sup>−</sup>), and HS<sup>−</sup> (magmatic fluids) are well documented in active hydrothermal systems. Since orogenic gold deposits form at greater depths in the crust, direct quantification of the chemistry of active mineralizing fluids is still lacking [31].

The difficulties related to analysis and experiments constitute other reasons. The fluid inclusions are the only witnesses of the fluids involved, and their analyses are limited by their micron-scale sizes. Until recently, Raman spectrometry was the only method for studying volatile composition, but it showed limited capacity for identification of hydrocarbons heavier than CH<sub>4</sub> [92]. Fluid inclusions are also analyzed by LA-ICP-MS, but elemental compositions are not informative for identifying metal complexes [65–67]. The solution lies in the use of techniques for studying oil inclusions, such as fluorescence and infrared spectroscopic techniques [93].

Carbonaceous organic matter occurs under various phases and forms, where its fine characterization is mostly restricted to petroleum and coal geology. As a consequence, few studies have integrated the complete link between various forms of organic matter and metals to decipher hydrothermal ore concentrating processes. The study of Dill et al. [85], integrating the concentration of sulfides and oxides with the interaction of silicates and organic matters, is an example of the next step to reach for defining the complex role of organic matter for the formation of orogenic gold deposits.

The complexity of reproducing experimental hydrothermal conditions is also challenging, as natural fluids are complex. Documenting gold solubility for a simple 1 or 2 component fluid at specific temperatures and pressures, although technically challenging, is relatively simple (e.g., [94]). However, it is not simple to determine the gold species

solubilized in a natural organic-bearing, multi-component fluid at high pressure and temperature. A major challenge will be applying organic component identification techniques for determining gold-carrying molecules formed at high temperature and pressure.

The importance of organic matter for concentrating gold constitutes a paradigm shift for geologists. This shift opens new research avenues requiring more multidisciplinary approaches. The finality will provide a better understanding of unique organic-metal ore-forming systems that range in age from Meso-Archean to modern. Hopefully, the outcome will have direct impacts on refining exploration models and conserving the gold supply for humanity.

**Funding:** This research received no external funding.

**Institutional Review Board Statement:** Not applicable.

**Informed Consent Statement:** Not applicable.

**Data Availability Statement:** Not applicable.

**Acknowledgments:** This review was possible because of the financial and logistical support of numerous exploration and mining companies worldwide. J. Walter and D. Genna (UQAC) provided comments to improve the first version.

**Conflicts of Interest:** The author declares no conflict of interest.

## References

- Klemm, D.; Klemm, R.; Murr, A. Gold of the Pharaohs—6000 years of gold mining in Egypt and Nubia. *J. Afr. Earth Sci.* **2001**, *33*, 643–659. [\[CrossRef\]](#)
- Coulson, M. Gold as an investment. *Appl. Earth Sci.* **2005**, *114*, 122–128. [\[CrossRef\]](#)
- Reuters Staff. Available online: <https://www.reuters.com/article/us-gold-mining-artisanal-explainer-idUSKBN1ZE0YU> (accessed on 20 March 2021).
- Phillips, G.N.; Powell, R. Formation of gold deposits: A metamorphic devolatilization model. *J. Metamorph. Geol.* **2010**, *28*, 689–718. [\[CrossRef\]](#)
- Wyman, D.A.; Cassidy, K.F.; Hollings, P. Orogenic gold and the mineral systems approach: Resolving fact, fiction and fantasy. *Ore Geol. Rev.* **2016**, *78*, 322–335. [\[CrossRef\]](#)
- Gaboury, D. Parameters for the formation of orogenic gold deposits. *Appl. Earth Sci.* **2019**, *128*, 124–133. [\[CrossRef\]](#)
- Groves, D.I.; Santosh, M.; Deng, J.; Wang, Q.; Yang, L.; Zhang, L. A holistic model for the origin of orogenic gold deposits and its implications for exploration. *Miner. Depos.* **2020**, *55*, 275–292. [\[CrossRef\]](#)
- Tomkins, A.G. On the source of orogenic gold. *Geology* **2013**, *41*, 1255–1256. [\[CrossRef\]](#)
- Groves, D. The crustal continuum model for late-Archaean lode-gold deposits of the Yilgarn Block, Western Australia. *Miner. Depos.* **1993**, *28*, 366–374. [\[CrossRef\]](#)
- Groves, D.I.; Goldfarb, R.J.; Robert, F.; Hart, C.J. Gold deposits in metamorphic belts: Overview of current understanding, outstanding problems, future research, and exploration significance. *Econ. Geol.* **2003**, *98*, 1–29.
- Fontboté, L.; Kouzmanov, K.; Chiaradia, M.; Pokrovski, G.S. Sulfide minerals in hydrothermal deposits. *Elements* **2017**, *13*, 97–103. [\[CrossRef\]](#)
- Craw, D.; Campbell, J.R. Tectonic and structural setting for active mesothermal gold vein systems, Southern Alps, New Zealand. *J. Struct. Geol.* **2004**, *26*, 995–1005. [\[CrossRef\]](#)
- Bradley, D.C. Secular trends in the geologic record and the supercontinent cycle. *Earth-Sci. Rev.* **2011**, *108*, 16–33. [\[CrossRef\]](#)
- Goldfarb, R.J.; Bradley, D.; Leach, D.L. Secular variations in economic geology. *Econ. Geol.* **2010**, *105*, 459–466. [\[CrossRef\]](#)
- Tomkins, A.G. A biogeochemical influence on the secular distribution of orogenic gold. *Econ. Geol.* **2013**, *108*, 193–197. [\[CrossRef\]](#)
- Large, R.R.; Gregory, D.D.; Steadman, J.A.; Tomkins, A.G.; Lounejeva, E.; Danyushevsky, L.V.; Halpin, J.A.; Maslennikov, V.; Sack, P.J.; Mukerjee, I.; et al. Gold in the oceans through time. *Earth Planet. Sci. Lett.* **2015**, *428*, 139–150. [\[CrossRef\]](#)
- Large, R.R.; Halpin, J.A.; Danyushevsky, L.V.; Maslennikov, V.V.; Bull, S.W.; Long, J.A.; Gregory, D.D.; Lounejeva, E.; Lyons, T.W.; Sack, P.J.; et al. Trace element content of sedimentary pyrite as a new proxy for deep-time ocean–atmosphere evolution. *Earth Planet. Sci. Lett.* **2014**, *389*, 209–220. [\[CrossRef\]](#)
- Lyons, T.W.; Gill, B.C. Ancient Sulfur Cycling and Oxygenation of the Early Biosphere. *Elements* **2010**, *6*, 93–99. [\[CrossRef\]](#)
- Pitcairn, I.K.; Olivo, G.R.; Teagle, D.A.H.; Craw, D. Sulfide evolution during prograde metamorphism of the Otago and Alpine Schists, New Zealand. *Can. Miner.* **2010**, *48*, 1267–1295. [\[CrossRef\]](#)
- Thomas, H.V.; Large, R.R.; Bull, S.W.; Maslennikov, V.; Berry, R.F.; Fraser, R.; Froud, S.; Moye, R. Pyrite and pyrrhotite textures and composition in sediments, laminated quartz veins, and reefs at Bendigo gold mine, Australia: Insights for ore genesis. *Econ. Geol.* **2011**, *106*, 1–31. [\[CrossRef\]](#)

21. Large, R.R.; Bull, S.W.; Maslennikov, V.V. A carbonaceous sedimentary source-rock model for Carlin-type and orogenic gold deposits. *Econ. Geol.* **2011**, *106*, 331–358. [\[CrossRef\]](#)
22. Finch, E.G.; Tomkins, A.G. Pyrite-pyrrhotite stability in a metamorphic aureole: Implications for orogenic gold genesis. *Econ. Geol.* **2017**, *112*, 661–674. [\[CrossRef\]](#)
23. Tomkins, A.G. Windows of metamorphic sulfur liberation in the crust: Implications for gold deposit genesis. *Geochim. Cosmochim. Acta* **2010**, *74*, 3246–3259. [\[CrossRef\]](#)
24. Williams-Jones, A.E.; Bowell, R.J.; Migdisov, A.A. Gold in solution. *Elements* **2009**, *5*, 281–287. [\[CrossRef\]](#)
25. Phillips, G.N.; Evans, K.A. Role of CO<sub>2</sub> in the formation of gold deposits. *Nature* **2004**, *429*, 860–863. [\[CrossRef\]](#) [\[PubMed\]](#)
26. Goldfarb, R.J.; Groves, D.I. Orogenic gold: Common vs evolving fluid and metal sources through time. *Lithos* **2015**, *223*, 2–26. [\[CrossRef\]](#)
27. Gorczyk, W.; Gonzalez, C.M.; Hobbs, B. Carbon dioxide as a proxy for orogenic gold source. *Ore Geol. Rev.* **2020**, *127*, 103829. [\[CrossRef\]](#)
28. Lang, J.R.; Baker, T. Intrusion-related gold systems: The present level of understanding. *Miner. Depos.* **2001**, *36*, 477–489. [\[CrossRef\]](#)
29. Augustin, J.; Gaboury, D. Multi-stage and multi-sourced fluid and gold in the formation of orogenic gold deposits in the world-class Mana district of Burkina Faso—Revealed by LA-ICP-MS analysis of pyrites and arsenopyrites. *Ore Geol. Rev.* **2019**, *104*, 495–521. [\[CrossRef\]](#)
30. Ridley, J.R.; Diamond, L.W. Fluid chemistry of orogenic lode gold deposits and implications for genetic models. *Rev. Econ. Geol.* **2000**, *13*, 146–162.
31. Yardley, B.W.D.; Bodnar, R.J. Fluids in the continental crust. *Geochem. Perspect.* **2014**, *3*, 1–127. [\[CrossRef\]](#)
32. Prokofiev, V.Y.; Naumov, V.B. Physicochemical parameters and geochemical features of ore-forming fluids for orogenic gold deposits throughout geological time. *Minerals* **2020**, *10*, 50. [\[CrossRef\]](#)
33. Elmer, F.L.; White, R.W.; Powell, R. Devolatilization of metabasic rocks during greenschist–amphibolite facies metamorphism. *J. Metam. Geol.* **2006**, *24*, 497–513. [\[CrossRef\]](#)
34. Gretchen, L.; Früh-Green, G.L. Fluids in metamorphism: Alteration of the oceanic lithosphere and implications for seafloor processes. *Elements* **2010**, *6*, 173–178.
35. Gaboury, D. Does gold in orogenic deposits come from pyrite in deeply buried carbon-rich sediments?: Insight from volatiles in fluid inclusions. *Geology* **2013**, *41*, 1207–1210. [\[CrossRef\]](#)
36. Chi, G.; Dubé, B.; Williamson, K.; Williams-Jones, A.E. Formation of the Campbell-Red Lake gold deposit by H<sub>2</sub>O-poor, CO<sub>2</sub>-dominated fluids. *Miner. Depos.* **2006**, *40*, 726–741. [\[CrossRef\]](#)
37. Mumm, A.S.; Oberthür, T.; Vetter, U.; Blenkinsop, T.G. High CO<sub>2</sub> content of fluid inclusions in gold mineralisations in the Ashanti Belt, Ghana: A new category of ore forming fluids? *Miner. Depos.* **1997**, *32*, 107–118. [\[CrossRef\]](#)
38. Klemd, R.; Hirdes, W. Origin of an unusual fluid composition in Early Proterozoic Palaeoplacer and lode-gold deposits in Birimian greenstone terranes of West Africa. *S. Afr. J. Geol.* **1997**, *100*, 405–414.
39. Gaboury, D.; Genna, D.; Trottier, J.; Bouchard, M.; Augustin, J.; Malcolm, K. The Perron gold deposit, Archean Abitibi belt, Canada: Exceptionally high-grade mineralization related to higher gold-carrying capacity of hydrocarbon-rich fluids. *Minerals* **2021**, in press.
40. Oliver, N.H.S.; Allibone, A.; Nugus, M.J.; Vargas, C.; Jongens, R.; Peattie, R.; Chamberlain, V.A. The Super-Giant, High Grade, Paleoproterozoic Metasedimentary Rock—and Shear-Vein-Hosted Obuasi (Ashanti) Gold Deposit, Ghana, West Africa. *Econ. Geol.* **2021**, *116*, 1329–1353. [\[CrossRef\]](#)
41. Pigois, J.P.; Groves, D.I.; Fletcher, I.R.; McNaughton, N.J.; Snee, L.W. Age constraints on Tarkwaian palaeoplacer and lode-gold formation in the Tarkwa-Damang district, SW Ghana. *Miner. Depos.* **2003**, *38*, 695–714. [\[CrossRef\]](#)
42. Gaboury, D.; Nabil, H.; Ennaciri, A.; Maacha, L. Structural setting and fluid composition of gold mineralization along the central segment of the Keraf suture, Neoproterozoic Nubian Shield, Sudan: Implications for the source of gold. *Int. Geol. Rev.* **2020**. [\[CrossRef\]](#)
43. Gaboury, D.; Mackenzie, D.; Craw, D. Fluid volatile composition associated with orogenic gold mineralization, Otago Schist, New Zealand: Implications of H<sub>2</sub> and C<sub>2</sub>H<sub>6</sub> for fluid evolution and gold source. *Ore Geol. Rev.* **2021**, *133*, 104086. [\[CrossRef\]](#)
44. Goldfarb, R.J.; André-Mayer, A.-S.; Jowitt, S.M.; Mudd, G.M. West Africa: The World's premier paleoproterozoic gold province. *Econ. Geol.* **2017**, *112*, 123–143. [\[CrossRef\]](#)
45. Lüders, V.; Klemd, R.; Oberthür, T.; Plessen, B. Different carbon reservoirs of auriferous fluids in African Archean and Proterozoic gold deposits? Constraints from stable carbon isotopic compositions of quartz-hosted CO<sub>2</sub>-rich fluid inclusions. *Miner. Depos.* **2015**, *50*, 449–454. [\[CrossRef\]](#)
46. Frimmel, H.E. Earth's continental crustal gold endowment. *Earth Planet. Sci. Lett.* **2008**, *267*, 45–55. [\[CrossRef\]](#)
47. Sillitoe, R.H.; Thompson, J.F.H. Intrusion-related vein gold deposits: Types, tectono-magmatic settings and difficulties of distinction from orogenic gold deposits. *Res. Geol.* **1998**, *48*, 237–250. [\[CrossRef\]](#)
48. Pitcairn, I.K.; Craw, D.; Teagle, D.A.H. Metabasalts as sources of metals in orogenic gold deposits. *Miner. Depos.* **2015**, *50*, 373–390. [\[CrossRef\]](#)
49. Augustin, J.; Gaboury, D. Paleoproterozoic plume-related basaltic rocks in the Mana gold district in western Burkina Faso, West Africa: Implications for exploration and the source of gold in orogenic deposits. *Afr. J. Earth Sci.* **2017**, *129*, 17–30. [\[CrossRef\]](#)

50. Patten, C.G.C.; Pitcairn, I.K.; Molnár, F.; Kolb, J.; Beaudoin, G.; Guillemette, C.; Peillod, A. Gold mobilization during metamorphic devolatilization of Archean and Paleoproterozoic metavolcanic rocks. *Geology* **2020**. [\[CrossRef\]](#)
51. Large, R.; Thomas, H.; Craw, D.; Henne, A.; Henderson, S. Diagenetic pyrite as a source for metals in orogenic gold deposits, Otago Schist, New Zealand. *N. Z. J. Geol. Geophys.* **2012**, *55*, 137–149. [\[CrossRef\]](#)
52. Pitcairn, I.K.; Leventis, N.; Beaudoin, G.; Faure, S.; Guillemette, C.; Dubé, B. A metasedimentary source of gold in Archean orogenic gold deposits. *Geology* **2021**. [\[CrossRef\]](#)
53. Zhong, R.; Brugger, J.; Tomkins, A.G.; Chen, Y.; Li, W. Fate of gold and base metals during metamorphic devolatilization of a pelite. *Geochim. Cosmochim. Acta* **2015**, *171*, 338–352. [\[CrossRef\]](#)
54. Wu, Y.-F.; Evans, K.; Fisher, L.A.; Zhou, M.-F.; Hu, S.-Y.; Fougereuse, D.; Large, R.R.; Li, J.W. Distribution of trace elements between carbonaceous matter and sulfides in a sediment-hosted orogenic gold system. *Geochim. Cosmochim. Acta* **2020**, *276*, 345–362. [\[CrossRef\]](#)
55. Augustin, J.; Gaboury, D.; Crevier, M. The world-class Wona-Kona gold deposit, Burkina Faso. *Ore Geol. Rev.* **2016**, *78*, 667–672. [\[CrossRef\]](#)
56. Dubé, B.; Mercier-Langevin, P.; Ayer, J.; Pilote, J.-L.; Monecke, T. *Gold Deposits of the World-Class Timmins-Porcupine Camp, Abitibi Greenstone Belt, Canada*; Society of Economic Geologists Special Publication: Littleton, CO, USA, 2020; Volume 23, pp. 53–80.
57. Gaboury, D.; Keita, M.; Guha, J.; Lu, H.-Z. Mass spectrometric analysis of volatiles in fluid inclusions decrepitated by controlled heating under vacuum. *Econ. Geol.* **2008**, *103*, 439–443. [\[CrossRef\]](#)
58. Whiticar, M.J. Carbon and hydrogen isotope systematics of bacterial formation and oxidation of methane. *Chem. Geol.* **1999**, *161*, 291–314. [\[CrossRef\]](#)
59. Canfield, D. A new model for Proterozoic ocean chemistry. *Nature* **1998**, *396*, 450–453. [\[CrossRef\]](#)
60. Steadman, J.A.; Large, R.R.; Blamey, N.J.; Mukherjee, I.; Corkrey, R.; Danyushevsky, L.V.; Maslennikov, V.; Hollings, P.; Garven, G.; Brand, U.; et al. Evidence for elevated and variable atmospheric oxygen in the Precambrian. *Precamb. Res.* **2020**, *343*, 105722. [\[CrossRef\]](#)
61. Heinson, G.; Duan, J.; Kirkby, A.; Robertson, K.; Thiel, K.; Aivazpourporgou, S.; Soyer, W. Lower crustal resistivity signature of an orogenic gold system. *Sci. Rep.* **2021**, *11*, 15807. [\[CrossRef\]](#)
62. Rickard, D.; Musmann, M.; Steadman, J.A. Sedimentary sulfide. *Elements* **2017**, *13*, 117–122. [\[CrossRef\]](#)
63. Stefansson, A.; Seward, T.M. Gold(I) complexing in aqueous sulphide solutions to 500 °C and 500 bar. *Geochim. Cosmochim. Acta* **2004**, *68*, 4121–4143. [\[CrossRef\]](#)
64. Simmons, S.F.; Tutolo, B.M.; Barker, S.L.L.; Goldfarb, R.J.; Robert, F. *Hydrothermal Gold Deposition in Epithermal, Carlin, and Orogenic Deposits*; Society of Economic Geologists Special Publication: Littleton, CO, USA, 2020; Volume 23, pp. 823–845.
65. Rauchenstein-Martinek, K.; Wagner, T.; Wälle, M.; Heinrich, C.A. Gold concentrations in metamorphic fluids: A LA-ICPMS study of fluid inclusions from the Alpine orogenic belt. *Chem. Geol.* **2014**, *385*, 70–83. [\[CrossRef\]](#)
66. Wagner, T.; Fusswinkel, T.; Wälle, M.; Heinrich, C.A. Microanalysis of fluid inclusions in crustal hydrothermal systems using laser ablation methods. *Elements* **2016**, *12*, 323–328. [\[CrossRef\]](#)
67. Fusswinkel, T.; Wagner, T.; Sakellaris, G. Fluid evolution of the Neoproterozoic Pampalo orogenic gold deposit (E Finland): Constraints from LA-ICPMS fluid inclusion microanalysis. *Chem. Geol.* **2017**, *450*, 96–121. [\[CrossRef\]](#)
68. Radtke, A.S.; Scheiner, B.J. Studies of hydrothermal gold deposition (I). Carlin gold deposit, Nevada: The role of carbonaceous materials in gold deposition. *Econ. Geol.* **1970**, *65*, 87–102. [\[CrossRef\]](#)
69. Crede, L.S.; Evans, K.A.; Rempel, K.U.; Brugger, J.; Etschmann, B.; Bourdet, J.; Reith, F. Revisiting hydrocarbon phase mobilization of Au in the Au–Hg McLaughlin Mine, Geysers/Clear Lake area, California. *Ore Geol. Rev.* **2020**, *117*, 103218. [\[CrossRef\]](#)
70. Emsbo, P.; Koenig, A.E. Transport of Au in Petroleum: Evidence from the Northern Carlin Trend, Nevada. In *Mineral Exploration and Research: Digging Deeper. Proc. 9th Biennial SGA Meeting*; Millpress: Dublin, Ireland, 2007; pp. 695–698.
71. Ge, X.; Selby, D.; Liu, J.; Chen, Y.; Cheng, G.; Shen, C. Genetic relationship between hydrocarbon system evolution and Carlin-type gold mineralization: Insights from Re–Os pyrobitumen and pyrite geochronology in the Nanpanjiang Basin, South China. *Chem. Geol.* **2021**, *559*, 119953. [\[CrossRef\]](#)
72. Fuchs, S.; Schumann, D.; Williams-Jones, A.E.; Vali, H. The growth and concentration of uranium and titanium minerals in hydrocarbons of the Carbon Leader Reef, Witwatersrand Supergroup, South Africa. *Chem. Geol.* **2015**, *393–394*, 55–66. [\[CrossRef\]](#)
73. Fuchs, S.; Williams-Jones, A.E.; Jackson, S.E.; Przybylowicz, W.J. Metal distribution in pyrobitumen of the Carbon Leader Reef, Witwatersrand Supergroup, South Africa: Evidence for liquid hydrocarbon ore fluids. *Chem. Geol.* **2016**, *426*, 45–59. [\[CrossRef\]](#)
74. Fuchs, S.; Schumann, D.; Martin, R.F.; Couillard, M. The extensive hydrocarbon-mediated fixation of hydrothermal gold in the Witwatersrand Basin, South Africa. *Ore Geol. Rev.* **2021**, *138*, 104313. [\[CrossRef\]](#)
75. Crede, L.S.; Evans, K.A.; Rempel, K.U.; Grice, K.; Sugiyama, I. Gold partitioning between 1-dodecanethiol and brine at elevated temperatures: Implications of Au transport in hydrocarbons for oil-brine ore systems. *Chem. Geol.* **2019**, *504*, 28–37. [\[CrossRef\]](#)
76. Crede, L.S.; Liu, W.; Evans, K.A.; Rempel, K.U.; Testemale, D.; Brugger, J. Crude oils as ore fluids: An experimental in-situ XAS study of gold partitioning between brine and organic fluid from 25 to 250 °C. *Geochim. Cosmochim. Acta* **2019**, *244*, 352–365. [\[CrossRef\]](#)
77. Liu, W.; Chen, M.; Yang, Y.; Mei, Y.; Etschmann, B.; Brugger, J.; Johannessen, B. Colloidal gold in sulphur and citrate-bearing hydrothermal fluids: An experimental study. *Ore Geol. Rev.* **2019**, *114*, 103142. [\[CrossRef\]](#)



- 
78. Petrella, L.; Thébaud, N.; Fougereuse, D.; Evans, K.; Quadir, Z.; Laflamme, C. Colloidal gold transport: A key to high-grade gold mineralization. *Miner. Depos.* **2020**, *55*, 1247–1254. [[CrossRef](#)]
  79. McLeish, D.F.; Williams-Jones, A.E.; Vasyukova, O.V.; Clark, J.R.; Board, W.S. Colloidal transport and flocculation are the cause of the hyperenrichment of gold in nature. *Proc. Natl. Acad. Sci. USA* **2021**, *118*, e2100689118. [[CrossRef](#)]
  80. Migdisov, A.; Guo, X.; Williams-Jones, A.; Sun, C.; Vasyukova, O.; Sugiyama, I.; Fuchs, S.; Pearce, K.; Roback, R. Hydrocarbons as ore fluids. *Geochem. Perspec. Lett.* **2017**, *5*, 47–52. [[CrossRef](#)]
  81. Tagirov, B.R.; Seward, T.M. Hydrosulfide/sulfide complexes of zinc to 250 °C and the thermodynamic properties of sphalerite. *Chem. Geol.* **2010**, *269*, 301–311. [[CrossRef](#)]
  82. Phillips, G.N.; Powell, R. Origin of Witwatersrand gold: A metamorphic devolatilisation—Hydrothermal replacement model. *Appl. Earth Sci.* **2011**, *120*, 112–129. [[CrossRef](#)]
  83. Hu, S.-Y.; Evans, K.; Fisher, L.; Rempel, K.; Craw, D.; Evans, N.J.; Cumberland, S.; Robert, A.; Grice, K. Associations between sulfides, carbonaceous material, gold and other trace elements in polyframboids: Implications for the source of orogenic gold deposits, Otago Schist, New Zealand. *Geochim. Cosmochim. Acta* **2016**, *180*, 197–213. [[CrossRef](#)]
  84. Hu, S.-Y.; Evans, K.; Craw, D.; Rempel, K.; Grice, K. Resolving the role of carbonaceous material in gold precipitation in metasediment-hosted orogenic gold deposits. *Geology* **2016**, *45*, 167–170. [[CrossRef](#)]
  85. Dill, H.G.; Kus, J.; Goldmann, S.; Suárez Ruiz, I.; Neumann, T.; Kaufhold, S. The physical-chemical regime of a sulfide-bearing semi-graphite mineral assemblage in metabasic rocks (SE Germany)—A multidisciplinary study of the missing link between impsonite and graphite. *Inter. J. Coal Geol.* **2019**, *214*, 103262. [[CrossRef](#)]
  86. Magoon, L.B.; Dow, W.G. *The Petroleum System—From Source to Trap*; American Association of Petroleum Geologists: Tulsa, OK, USA, 1994; Volume 60.
  87. Sherwood Lollar, B.; Westgate, T.; Ward, J.; Slater, G.F.; Lacrampe-Couloume, G. Abiogenic formation of alkanes in the Earth's crust as a minor source for global hydrocarbon reservoirs. *Nature* **2002**, *416*, 522–524. [[CrossRef](#)] [[PubMed](#)]
  88. Reeves, E.P.; Fiebig, J. Abiotic Synthesis of Methane and Organic Compounds in Earth's Lithosphere. *Elements* **2020**, *16*, 25–31. [[CrossRef](#)]
  89. Goldfarb, R.J.; Taylor, R.D.; Collins, G.S.; Goryachev, N.A.; Orlandini, O.F. Phanerozoic continental growth and gold metallogeny of Asia. *Gondwana Res.* **2014**, *25*, 48–102. [[CrossRef](#)]
  90. Savchuk, Y.S.; Asadulin, E.E.; Volkov, A.V.; Aristov, V.V. The Muruntau deposit: Geodynamic position and a variant of genetic model of the ore-forming system. *Geol. Ore Depos.* **2018**, *60*, 365–397. [[CrossRef](#)]
  91. Steele-MacInnis, S.; Manning, C.E. Hydrothermal properties of geologic fluids. *Elements* **2020**, *16*, 375–380. [[CrossRef](#)]
  92. Frezzotti, M.L.; Tecce, F.; Casagli, A. Raman spectroscopy for fluid inclusion analysis. *J. Geochem. Explor.* **2012**, *112*, 1–20. [[CrossRef](#)]
  93. Bourdet, J.; Eadington, P. *Fluorescence and Infrared Spectroscopy of Inclusion; Oil*. Internal Report EP129625 Australia; CSIRO: Canberra, Australia, 2012; p. 60.
  94. Zotov, A.V.; Kuzmin, N.N.; Reukov, V.L.; Tagirov, B.R. Stability of  $\text{AuCl}_2^-$  from 25 to 1000 °C at pressures to 5000 bar and consequences for hydrothermal gold mobilization. *Minerals* **2018**, *8*, 286. [[CrossRef](#)]